Applied Catalysis B: Environmental 242 (2019) 218–226

Contents lists available at ScienceDirect

Applied Catalysis B: Environmental

journal homepage: www.elsevier.com/locate/apcatb

Photocatalytic reduction of Cr(VI) on hematite nanoparticles in the presence of oxalate and citrate

Imme Kretschmer[a], Alejandro M. Senn[b], J. Martín Meichtry[b], Graciela Custo[c], Emilia B. Halac[d,e], Ralf Dillert[a], Detlef W. Bahnemann[a,f], Marta I. Litter[b,g,*]

[a] Institute of Technical Chemistry, Leibniz University Hannover, Callinstr. 3, D-30167, Hannover, Germany
[b] Gerencia Química, Comisión Nacional de Energía Atómica, CONICET, Av. Gral. Paz 1499, 1650, San Martín, Prov. de Buenos Aires, Argentina
[c] Gerencia Química, Comisión Nacional de Energía Atómica, Av. Gral. Paz 1499, 1650, San Martín, Prov. de Buenos Aires, Argentina
[d] Departamento Física de la Materia Condensada, Gerencia de Investigaciones y Aplicaciones, Comisión Nacional de Energía Atómica, Av. Gral. Paz 1499, 1650, San Martín, Prov. de Buenos Aires, Argentina
[e] Escuela de Ciencia y Tecnología, Universidad Nacional de San Martín, Martín de Irigoyen 3100, 1650, San Martín, Prov. de Buenos Aires, Argentina
[f] Laboratory for Nanocomposite Materials, Department of Photonics, Faculty of Physics, Saint-Petersburg State University, Ulianovskaia str. 3, Peterhof, Saint-Petersburg, 198504, Russia
[g] Instituto de Investigación e Ingeniería Ambiental, Universidad Nacional de General San Martín, Campus Miguelete, Av. 25 de Mayo y Francia, 1650, San Martín, Prov. de Buenos Aires, Argentina

ARTICLE INFO

Keywords:
Nanohematite
Cr(VI)
Photocatalysis
Oxalate
Citrate

ABSTRACT

Hematite nanoparticles (*n*Hm) were tested for Cr(VI) photocatalytic reduction (300 μM) in the presence of different electron donors such as citrate (Cit), oxalate (Ox), 2-propanol and methanol. At pH 3 and under irradiation at $\lambda \geq 310$ nm, almost negligible reaction took place in the absence of donor or with the alcohols, while the reduction was very rapid in the presence of Cit (less than 25 min), and faster with Ox (15 min). Homogeneous experiments with $FeCl_3$ instead of *n*Hm showed a complete Cr(VI) reduction in the presence of both complexing agents in less than 10 min. Under irradiation at $\lambda > 495$ nm and with *n*Hm at pH 3, a good Cr(VI) transformation took place with both donors, but at a considerably lower rate than under UV light (around 100% at 180 min), the decay being negligible in the homogeneous systems with Fe(III). Under irradiation at $\lambda > 610$ nm, no Cr(VI) transformation took place over *n*Hm. Experiments at pH 6 under UV–Vis light with Cit in the presence of *n*Hm gave a good Cr(VI) decay, faster with Fe(III) (60% and 90% in 105 min, respectively); some Cr(VI) transformation (around 35% in 180 min) was found with Cit under Vis light. Interestingly, at both wavelength ranges, the reaction was negligible when Ox was used. Mechanisms taking place under the different conditions were proposed, including the role of surface charge transfer complexes on *n*Hm.

1. Introduction

Chromium(VI) is well known as a very toxic, carcinogenic chemical species [1], present in waters coming mainly from anthropic sources due to its multiple industrial applications (e.g. metallurgy, paintings, textile industry, wood, etc.) [2], and constituting a priority pollutant in many countries. Several methods have been developed to remove Cr(VI) from polluted waters, mostly by reduction to Cr(III), which is an essential trace element in nutrition and considered to be nontoxic [3]. The guideline value for Cr(VI) in drinking water is 0.05 mg L^{-1} [1].

Cr(VI) removal by heterogeneous photocatalysis with TiO_2 and other semiconductors has been extensively studied, and a plethora of papers were published, especially by us, together with various reviews on the subject [3–9], where specific references can be consulted. The mechanism of photocatalytic reduction of Cr(VI) over TiO_2 has been thoroughly studied (see e.g. Refs. [5–14]). Cr(VI) reduction with this semiconductor proceeds through three successive one electron reactions of Cr(VI) with electrons of the conduction band (e_{CB}^-) generated after irradiation of the semiconductor. The fast photocatalytic reduction can be ascribed to the formation of a charge transfer (CT) complex between Cr(VI) and TiO_2, detected spectroscopically [15]. Attack of holes to adsorbed water or surface hydroxyl groups produce hydroxyl radicals ($HO^\cdot$); H_2O_2 is also proposed to be formed in the system.

* Corresponding author at: Gerencia Química, Comisión Nacional de Energía Atómica, CONICET, Av. Gral. Paz 1499, 1650, San Martín, Prov. de Buenos Aires, Argentina.

E-mail addresses: litter@cnea.gov.ar, marta.litter@gmail.com (M.I. Litter).

https://doi.org/10.1016/j.apcatb.2018.09.059
Received 4 May 2018; Received in revised form 11 September 2018; Accepted 17 September 2018
Available online 22 September 2018
0926-3373/

$$TiO_2 + h\nu \rightarrow e_{CB}^- + h_{VB}^+ \quad (1)$$

$$Cr(VI)/Cr(V)/Cr(IV) + e_{CB}^- \rightarrow Cr(V)/Cr(IV)/Cr(III) \quad (2)$$

$$H_2O_{ads}/OH_{surf}^- + h_{VB}^+ \rightarrow HO_{surf}^{\cdot} \quad (3)$$

$$2\ HO_{surf}^{\cdot} \rightarrow H_2O_2 \quad (4)$$

$$H_2O_2 + h_{VB}^+ \rightarrow HO_2^{\cdot} + H^+ \quad (5)$$

The addition of a sacrificial electron donor has a profound effect on the enhancement of the TiO_2 photocatalytic Cr(VI) transformation by capturing h_{VB}^+ and decreasing e_{CB}^-/h_{VB}^+ recombination. In the absence of donors, reduced Cr species can be reoxidized by $h_{VB}^+/HO^{\cdot}$ (Eq. (6)), but at high concentration of donors, reaction (7) will be preferred; alcohols and carboxylates have been tested as donors, among others. EDTA, oxalate (Ox) and, especially, citrate (Cit) have the ability to complex and to stabilize Cr(V), a proven intermediate in the reduction of Cr(VI) over TiO_2 [11–14]. Additionally, reducing radicals are usually formed by $h_{VB}^+/HO^{\cdot}$ generated in the photocatalytic processes, enhancing also the Cr(VI) photocatalytic reduction:

$$Cr(V)/Cr(IV)/Cr(III) + h_{VB}^+/HO^{\cdot} \rightarrow Cr(VI)/Cr(V)/Cr(IV) \quad (6)$$

$$Ox/Cit + h_{VB}^+/HO^{\cdot} \rightarrow Ox^{\cdot}/Cit^{\cdot} + H^+/H_2O \quad (7)$$

$$Ox^{\cdot}/Cit^{\cdot} + Cr(VI)/Cr(V)/Cr(IV) \rightarrow Cr(V)/Cr(IV)/Cr(III) + \text{oxid. products of Ox/Cit} \quad (8)$$

Hematite (α-Fe_2O_3) is an n-type semiconductor with a narrow band gap (E_g = 2.0–2.3 eV); the conduction band (CB) and valence band (VB) edge positions are in the range 0.0–0.6 and 2.3–2.7 V,[1] respectively, and the material presents very low electron and hole mobility (about $10^{-2}\ cm^2\ V^{-1}\ s^{-1}$) [16,17 and references therein]. Consequently, because of the narrowness of d-bands and the low mobility of holes, the poor conductivity and the short-hole diffusion length, α-Fe_2O_3 has poor photocatalytic properties [18–20].

On the other hand, due to the narrow bandgap, α-Fe_2O_3 can be utilized to absorb visible light, making possible the use of a substantial fraction of the solar spectrum. Kormann et al. [18] concluded that α-Fe_2O_3 is photocatalytically active in oxidations only in the cases where the compound is a strong reducing or complexing agent.

However, many papers on α-Fe_2O_3 claiming its potential use as photocatalyst under UV or visible light for water or air decontamination have been published (see e.g. [20–35]), including the enhancement of the reaction by Ox [36], although the photocatalytic treatment of inorganic pollutants using nanoparticulated hematite has been scarcely studied. In their recent review on hematite as photocatalyst, Mishra and Chun [20] only mention Ag^+ reduction to Ag° as application. Mekatel et al. [37] found a remarkable performance of nanosized α-Fe_2O_3 supported on a clay for Cr(VI) reduction under visible and solar light. The photocatalytic Cr(VI) reduction was seldom cited: the reaction under visible light was enhanced 9-fold with α-Fe_2O_3 nanoparticles deposited onto a graphite oxide carbon compared with pure α-Fe_2O_3 [38], and Cr(VI) removal with zerovalent iron nanoparticles (nZVI) [39] was enhanced by UV–Vis irradiation, with active wavelengths in the visible range with the photocatalytic process promoted by the external iron oxides of the nanoparticles acting as semiconductors [40].

According to the above indicated lack of work devoted to iron oxides as photocatalysts for transformation of inorganic pollutants and their scarcely explored potentiality, especially under visible light, a study with hematite nanoparticles (*n*Hm) for photocatalytic reduction of Cr(VI) under UV and visible light was judged interesting and has been undertaken in this paper, focused on the effect of the presence of different electron donors, the irradiation wavelength and the working pH.

[1] All redox potentials are at pH 0 vs. SHE.

2. Experimental

2.1. Chemicals

Cr(VI) ($K_2Cr_2O_7$, 99.9% Merck), Cit ($C_6H_8O_7{\cdot}H_2O$, 99% Riedel de Häen), Ox ($C_2H_2O_4{\cdot}H_2O$, 99%, Merck), 2-PrOH (C_3H_8O, 99%, Biopack), MeOH (CH_3OH, 99%, Biopack) were used. All other chemicals were reagent grade. $HClO_4$ (70%) was Merck. In all the experiments, Milli-Q water was used (resistivity = 18 MΩ.cm). α-Fe_2O_3 nanoparticles (*n*Hm, 20–30 nm) were produced via controlled hydrolysis of $FeCl_3$ followed by membrane dialysis and freeze-drying of the resulting transparent solution, according to previous references [18,41].

2.2. Irradiation procedure

All experiments were carried out at 25 °C in a thermostatted cylindrical glass cell (i.d. = 32 mm, height = 90 mm) provided with magnetic stirring and a Teflon cap with a sampler and a light filter holder; the system was open to the atmosphere. A high-pressure xenon arc lamp (Osram XBO, 450 W) with a water IR filter was used to irradiate the cell. A collimated light beam, 18 mm diameter, entered the cell through the cut-off filter from the top. Three different cut-off filters were used: a UV–Vis filter for $\lambda \geq 310$ nm (glass-borosilicate), a Vis filter for $\lambda \geq 495$ nm (GG 495) and a GG 610 cut-off filter for $\lambda \geq 610$ nm. The incident photon flux per unit volume ($q^{\circ}_{n,p}/V$) obtained with the UV–Vis filter was 20.4 μeinstein $s^{-1}\ L^{-1}$, as determined by ferrioxalate actinometry in the same conditions as those of the photocatalytic experiments. UV–Vis photon fluxes through the reactor of 84.4, 60.2 and 26.8 μeinstein $s^{-1}\ L^{-1}$ were calculated for the glass-borosilicate, the GG 495 and the GG 610 filter, respectively; the details of these calculations, as well as the spectra, can be found in Figs. S1 and S2, section S1 (Appendix A, Supplementary Data).

For each photocatalytic run, a fresh aqueous suspension (30 mL) containing *n*Hm (3 mM, 0.48 g L^{-1}), Cr(VI) (300 μM) and the donor at the corresponding concentration was prepared and adjusted to pH 3 with dilute $HClO_4$ or to pH 6 with concentrated NaOH. The suspension was ultrasonicated for 2 min, filled into the reaction cell and stirred magnetically in the dark for 30 min to assure the adsorption equilibrium of the components of the mixture onto the hematite surface. Then, irradiation was started for the indicated time. As donors, 2-PrOH (0.1 M), MeOH (0.1 M), Cit (2 mM) and Ox (2 mM) were tested. Leaching of Fe into solution was observed and measured. Experiments with Fe(III) in solution (absence of *n*Hm) were performed under the same conditions, adding $FeCl_3$ at a concentration equal to the highest total Fe (Fe_T) concentration measured in the solution during the equivalent experiment with *n*Hm (see below). After irradiation, significant changes were only observed with Ox, either in the heterogeneous or in the homogeneous systems, where the pH changed from 3 to 5. Control reactions in the dark were also carried out. Similar experiments were performed using an initial pH of 6, without changes in pH at the end of the irradiation.

2.3. Analysis of samples

For Cr(VI), Fe(II) and Fe_T analysis, samples (1 mL) of the different runs were taken periodically in Eppendorf tubes and centrifuged for 5 min at 13,400 rpm using an Eppendorf MiniSpin® centrifuge. Cr(VI) concentration was followed in the supernatant by the spectrophotometric diphenylcarbazide method [42], measuring at 540 nm. Analysis of Fe(II) and Fe_T in solution was done similarly by spectrophotometric determination of the 1,10-phenanthroline-Fe(II)-complex at 508 nm [43].

UV–Vis absorption measurements for Cr(VI) and Fe(II)/Fe_T quantification were performed employing a UV–Vis T80+ spectrophotometer (PG instruments Ltd). All spectra of the solutions were obtained with a Hewlett-Packard diode array UV–Vis, model HP 8453. *n*Hm colloidal

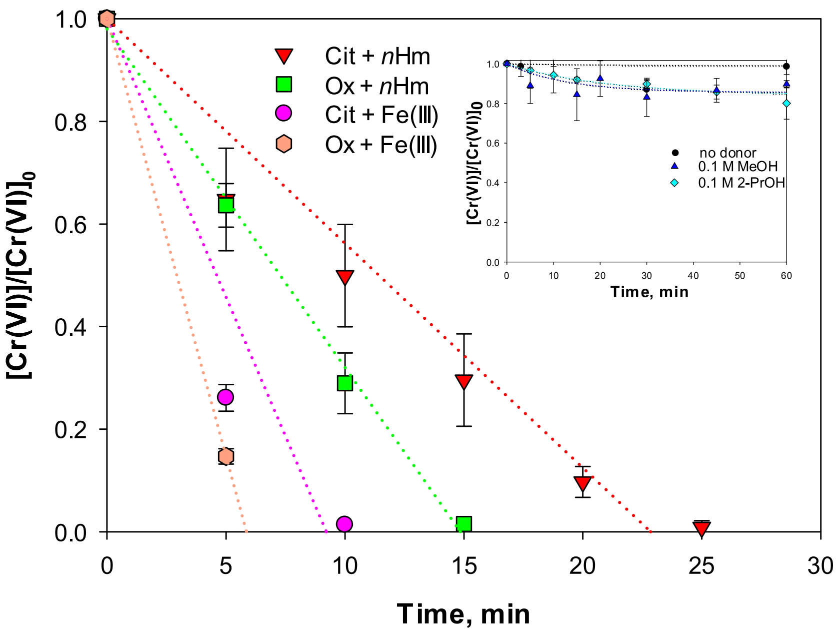

Fig. 1. Evolution of normalized Cr(VI) concentration in the presence of Cit or Ox over *n*Hm or with Fe(III) in solution under $\lambda > 310$ nm at pH 3. Inset: evolution of normalized Cr (VI) concentration over *n*Hm without donors or in the presence of 0.1 M 2-PrOH or 0.1 M MeOH over *n*Hm under $\lambda > 310$ nm. Conditions: [Cr(VI)] = 300 μM, [*n*Hm] = 0.48 g L^{-1}, [Cit] = [Ox] = 2 mM, [Fe(III)] = 53 μM for Cit, [Fe(III)] = 114 μM for Ox, $q^{\circ}_{n,p}/V$ = 84.4 μeinstein s^{-1} L^{-1}, T = 24 °C. Dotted lines are only for a better visualization and do not correspond to any fitting model.

suspensions spectra were measured with an integrating sphere (ISR-603) attached to a Shimadzu UV-3600Plus spectrophotometer.

Total chromium (Cr_T) in solution was measured by Total Reflection X-ray Fluorescence (TXRF) with the S2 PICOFOX spectrometer from Bruker.

The samples for Raman characterization were prepared as follows. A suspension (30 mL) containing *n*Hm (0.48 g L^{-1}), Cr(VI) (300 μM), Cit (2 mM) or Ox (2 mM) and adjusted to pH 6 with dilute NaOH was irradiated for 2 h with the high-pressure xenon arc lamp as described in Section 2.2. The solution was filtered using a vacuum system with a nylon filter (Osmonics, 0.22 μm pore size, 47 mm diameter). The filter membrane with the retained solid was dried overnight in a vacuum desiccator at room temperature. Raman spectra of the obtained solid were recorded with a LabRAM HR Raman system (Horiba Jobin Yvon), equipped with two monochromator gratings and a charge coupled device detector. The He-Ne laser line at 632.8 nm was used as the excitation source.

3. Results

3.1. Photocatalytic experiments under UV–Vis irradiation at pH 3

Fig. 1 shows the normalized Cr(VI) concentration temporal profiles of experiments with 300 μM Cr(VI) at pH 3 in the presence of 2 mM Cit and 2 mM Ox over *n*Hm (0.48 g L^{-1}) under UV–Vis irradiation ($\lambda > 310$ nm) after 30 min of stirring in the dark. Similar experiments in a homogeneous system composed of dissolved Fe(III) and both ligands under UV–Vis irradiation are included. The photocatalytic Cr(VI) reduction over TiO_2 is not dependent on the presence of oxygen (e.g., [3]), and, for this reason, all experiments have been performed with the reactor open to the air (see however, Section 4 about the reduction of O_2 by e_{CB}^- of *n*Hm). The initial Fe concentration used in these experiments was the maximum [Fe_T] (added as Fe(III)) obtained in the experiments with *n*Hm (see Fig. 2, i.e., 53 μM for Cit and 114 μM for Ox). The inset shows similar experiments with *n*Hm without donors, and with 0.1 M 2-PrOH and 0.1 M MeOH.

Fig. 1 shows that Ox and Cit were efficient donors: with Cit, a complete Cr(VI) decay could be seen after 25 min of irradiation, while with Ox the reaction was even faster (complete Cr(VI) decay after 15 min). Without donors, the decay was negligible and, with the alcohols, only a small Cr(VI) reduction was observed (10 and 20% for MeOH and 2-PrOH, respectively, after 180 min). In the absence of *n*Hm or Fe(III), the photoreduction of Cr(VI) did not take place (not shown). Fig. 1 indicates that the homogeneous experiments with Fe(III) in solution, using an Fe(III) concentration equal to the highest [Fe_T] determined during the experiment with *n*Hm and either Cit or Ox (see Fig. 2), are more efficient for Cr(VI) removal than those in the presence of *n*Hm. Dark experiments (section S2, Fig. S3) indicate a small ($\approx$17%) decay of Cr(VI) in the absence of the donors, similar to that obtained in the presence of 2-PrOH and MeOH (not shown). This decay can be ascribed to adsorption of Cr(VI) onto *n*Hm. In the presence of 2 mM Cit or Ox, the decay was somewhat smaller (10 and 14% for Cit and Ox, respectively), which can probably be due to competitive adsorption between the carboxylates and Cr(VI). No significant additional Cr(VI) decay could be appreciated in any case after 30 min stirring in the dark (even after 180 min). In all cases, no significant changes of [Cr_T] were obtained, indicating that all formed Cr(III) remained in solution.

After 30 min stirring in the dark, the initial [Fe_T] was almost identical and around 20 μM for both Cit and Ox. The amount of dissolved Fe_T stayed constant around 20 μM for Cit, while for Ox, a continuous increase in [Fe_T] took place all throughout the experiment (up to 60 min). Under irradiation, [Fe_T] reaches values higher than in the dark for both ligands. A continuous increase of [Fe_T], up to not very high values (53 μM at 60 min, i.e. 1.8% of the initial iron oxide) was observed for Cit, while for Ox, higher values were reached, with the maximum concentration (114 μM, i.e., 3.8% of the initial iron oxide) observed at 30 min, and a decrease at longer times. This decrease can be ascribed to the increase in pH of the solution from 3 to 5 at t = 45 min, which decreases the Fe(III) solubility. Fe(II) was only observed under irradiation, and only once Cr(VI) has been completely reduced, i.e., after around 15 and 25 min for Ox and Cit, respectively (cf. Figs. 1 and 2(a)). This was expected because of the rapid reaction of Fe(II) with Cr (VI) at pH 3 [44]. In the experiments with Cit, after an important increase at around 30 min, Fe(II) reaches a steady state value (ca. 20 μM), while [Fe_T] is slowly growing throughout the reaction time, indicating an increase of the concentration of soluble Fe(III) complexes. In the experiments with Ox, Fe(II) follows the same behavior of [Fe_T], increasing from 0 at 10 min until 52 μM at 30 min; the decrease in [Fe(II)] observed at longer times can be ascribed to the oxidation of Fe(II) by O_2 (faster at pH 5 than at pH 3 [45]).

The evolution of [Fe(II)] in solution for the homogeneous systems is displayed in Fig. 2(b), and compared with the values obtained in the

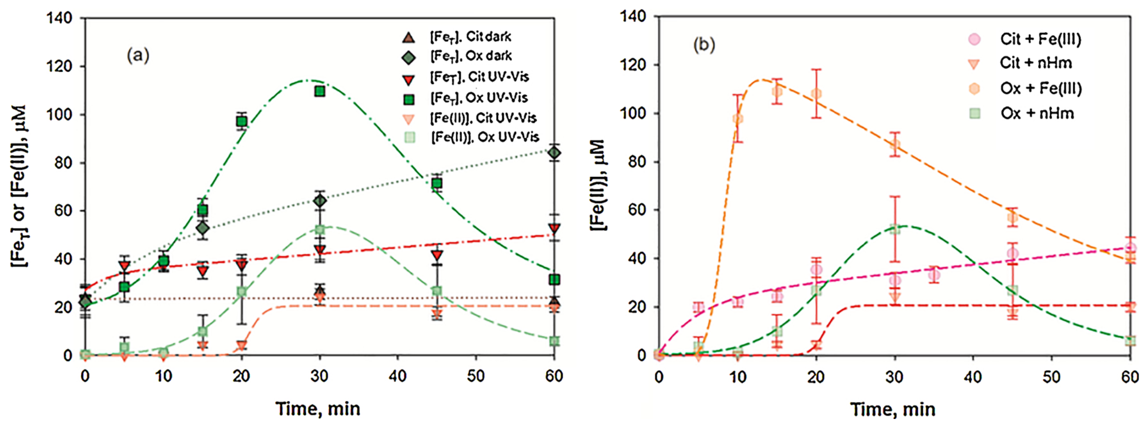

Fig. 2. (a) Evolution of [Fe$_T$] and [Fe(II)] during the photocatalytic reduction of Cr(VI) with *n*Hm under λ > 310 nm at pH 3; the dark reaction is also shown. (b) Evolution of [Fe(II)] during the photochemical reduction of Cr(VI) with dissolved Fe(III) compared with the experiments over *n*Hm. Dark symbols and dotted lines: [Fe$_T$] in the dark; dark symbols and dotted-dashed lines: [Fe$_T$] under UV–Vis irradiation; light symbols and dashed lines: [Fe(II)] under UV–Vis irradiation. Conditions of Fig. 1. Lines are only for a better visualization and do not correspond to any fitting model. Note that t = 0 implies a previous dark period of 30 min (not shown) for all the curves.

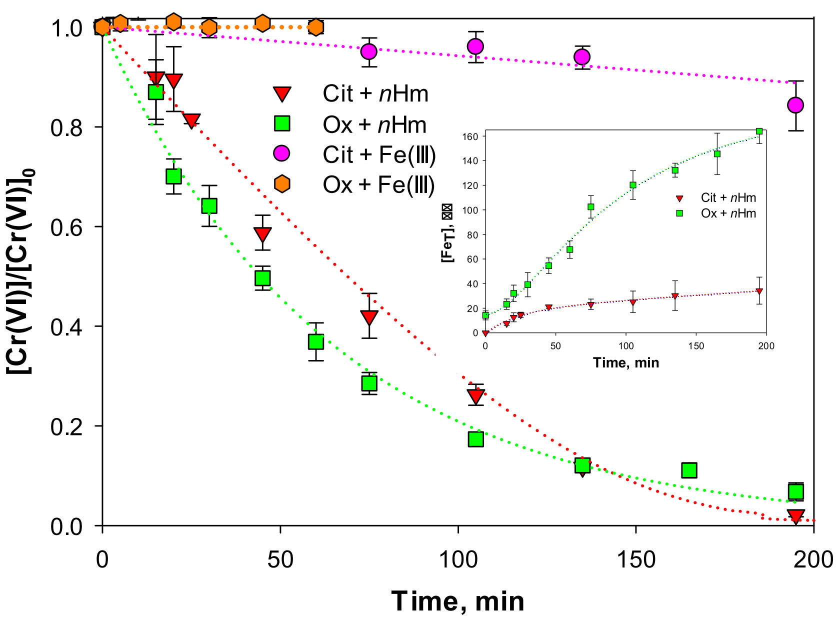

Fig. 3. Evolution of normalized Cr(VI) concentration during the photodegradation with *n*Hm or with Fe(III) in solution under λ > 495 nm at pH 3. Inset: evolution of [Fe$_T$] during the reaction with *n*Hm. Conditions: [Cr(VI)] = 300 µM, [*n*Hm] = 0.48 g L^{-1}, [Cit] = [Ox] = 2 mM, [Fe(III)] = 34 µM for Cit, [Fe(III)] = 164 µM for Ox, $q°_{n,p}/V$ = 60.2 µeinstein s^{-1} L^{-1}, T = 24 °C. Dotted lines are only for a better visualization and do not correspond to any fitting model.

heterogeneous systems. For Cit, a small amount of Fe(II) (20 µM) was detected at 5 min in the homogeneous system, i.e., faster than in the presence of *n*Hm, and, since this point, [Fe(II)] increased steadily until 44 µM at 60 min, i.e., when more than 80% of the initial Fe(III) was reduced. As said, pH was almost constant during the Cit experiments. In both systems with Ox, a maximum [Fe(II)] is observed; however, the maximum is reached faster in the homogeneous system (around 10–15 min), correspondingly with the faster Cr(VI) removal (Fig. 1). A decrease at longer times was observed in both Ox systems, ascribed, as said, to Fe(II) reoxidation to Fe(III) by O_2 and Fe(III) precipitation due to the increase in pH.

3.2. Photocatalytic experiments under visible irradiation at pH 3

Fig. 3 shows the Cr(VI) normalized concentration profiles of experiments at pH 3 under visible irradiation (λ > 495 nm). The inset shows the evolution of [Fe$_T$] during the experiments with *n*Hm. The results with the photocatalyst indicate a much slower Cr(VI) reduction than under λ > 310 nm (cf. Figs. 1 and 3), with an almost complete reduction only after 3 h in the presence of both ligands, although the reaction was initially faster with Ox. However, the decrease of the rate of Cr(VI) decay was far more noticeable in the homogeneous systems ([Fe(III)] = 34 µM for Cit, [Fe(III)] = 164 µM for Ox, i.e., corresponding to the maximum [Fe$_T$] measured for the experiments with *n*Hm, see inset of Fig. 3), where an almost negligible reaction was observed after 180 min of irradiation. [Fe$_T$] in solution was much higher for both donors than under dark conditions (see Fig. 2(a)), indicating that visible irradiation clearly contributes to Fe dissolution. Similarly to the experiments under UV–Vis irradiation, [Fe$_T$] in solution was much higher for Ox (164 µM) than for Cit (34 µM), but more Fe is dissolved compared with the experiments under UV–Vis irradiation, probably due to the slower reaction and longer irradiation time and contact time with *n*Hm. No Fe(II) could be found in solution in any case, because Cr(VI) disappears only at the end of the irradiation, and thus it constantly oxidizes the Fe(II) formed during the reaction. In the homogeneous reaction, [Fe$_T$] in solution is always constant (164 µM for Ox and 34 µM for Cit, not shown). As observed under UV–Vis irradiation, no significant changes were obtained in [Cr$_T$] at the end of the experiments,

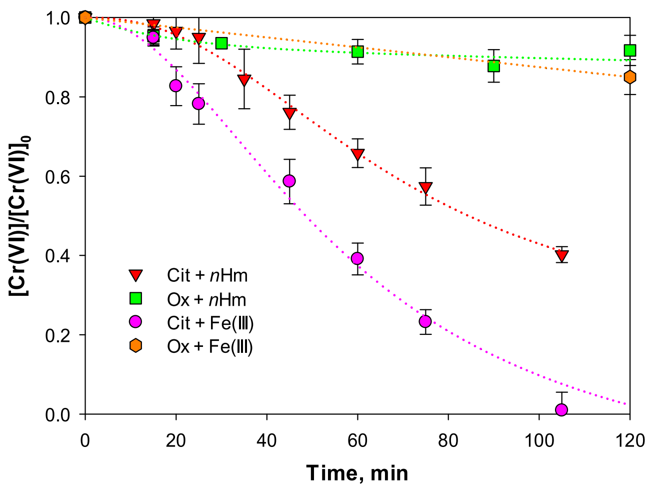

Fig. 4. Evolution of normalized concentration of Cr(VI) over *n*Hm or with Fe (III) in the presence of Cit or Ox under $\lambda > 310$ nm at pH 6. Conditions: [Cr (VI)] = 300 μM, [*n*Hm] = 0 or 0.48 g L^{-1}, [Cit] = [Ox] = 2 mM, [Fe (III)] = 13 μM, $q^{\circ}_{n,p}/V$ = 84.4 μeinstein s^{-1} L^{-1}, *T* = 24 °C. Dotted lines are only for a better visualization and do not correspond to any fitting model.

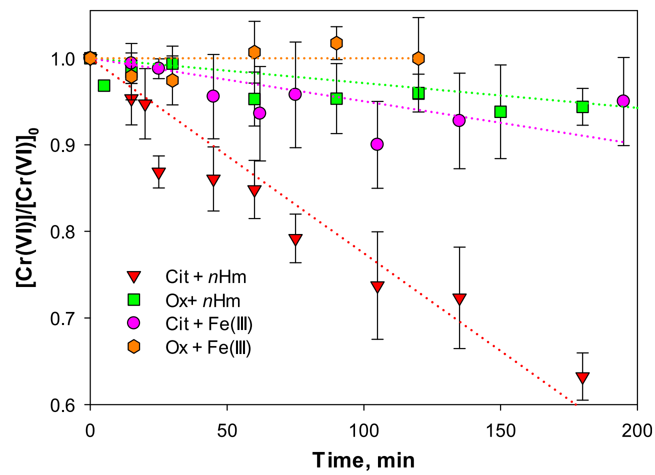

Fig. 5. Evolution of normalized concentration of Cr(VI) over *n*Hm or with Fe (III), in the presence of Cit or Ox, under $\lambda > 495$ nm at pH 6. Conditions: [Cr (VI)] = 300 μM, [*n*Hm] = 0 or 0.48 g L^{-1}, [Cit] = [Ox] = 2 mM, [Fe (III)] = 13 μM, $q^{\circ}_{n,p}/V$ = 60.2 μeinstein s^{-1} L^{-1}, *T* = 24 °C. Dotted lines are only for a better visualization and do not correspond to any fitting model.

indicating that all formed Cr(III) remained in solution.

No Cr(VI) decay was observed under the conditions of Fig. 3 when the GG 610 filter was used.

3.3. Photocatalytic experiments under UV–Vis and Vis irradiation at pH 6

Fig. 4 shows the results of experiments under UV–Vis irradiation at pH 6. For the homogeneous system, an initial [Fe(III)] of 13 μM was used for all experiments; this value was chosen because the maximum [Fe_T] measured for each donor in the heterogeneous reaction was quite low and similar under both UV–Vis and Vis irradiation (from 15 to 6 μM for Cit and Ox, respectively, see below). The Cr(VI) decay over *n*Hm was considerably slower than that obtained at pH 3 (cf. Figs. 1 and 4), with only 60% of the initial Cr(VI) being reduced in 105 min in the presence of Cit and almost negligible decay (ca. 14% at 240 min, not shown) with Ox. Similar results were obtained when using Fe(III) instead of *n*Hm: with Cit, the homogeneous reaction was more rapid than when using *n*Hm, being complete in around 100 min, but also very much slower than at pH 3; only 15% Cr(VI) removal was obtained with Ox. The results indicate that, at this pH, and in both heterogeneous and homogeneous systems, Cit is a more effective donor than Ox. A 32% decrease of [Cr_T] in solution was obtained at the end of the experiment with Cit, indicating that the formed Cr(III) is partially retained in the *n*Hm surface; as expected, no change of [Cr_T] in solution was measured in the experiment with Ox.

The amount of Cr(VI) removed during the first 30 min in the dark experiments in the presence of either Ox or Cit (not shown) was very similar to that obtained at pH 3 (14% with Ox, 9% with Cit), with no significant additional decay even after 180 min; it can also be ascribed to adsorption of Cr(VI) onto *n*Hm. For both donors, [Fe_T] increased steadily from an initial value of 6 μM to 15 μM and 10 μM after 180 min for Cit and Ox, respectively.

Fig. 5 shows the results at pH 6 under Vis irradiation. It can be observed that Cr(VI) reduction only takes place importantly in the presence of Cit and *n*Hm (37% at 180 min), and that the reaction in the presence of Ox is almost negligible, similarly to that observed at the same pH under UV–Vis irradiation; the homogeneous reactions with dissolved Fe(III) (13 μM for both, Ox and Cit) were also negligible.

All iron found in solution after the heterogeneous reaction was as Fe (III), and Fe(II) was never detected. [Fe_T] variation was negligible for Ox, with a rather constant value around 6 μM, while, for Cit, [Fe_T] increased from 6 μM to 13 μM after 180 min. It was concluded that *n*Hm photodissolution in the presence of Cit and, especially, Ox, is negligible under these conditions. In any case, changes in [Cr_T] in solution were never detected, even for the *n*Hm-Cit system, where a significant decrease of [Cr(VI)] was appreciated.

4. Discussion

4.1. Proposed mechanisms

If the mechanism of Eqs. (1)–(5) is applied to reactions with *n*Hm [17,35], results of Fig. 1 show that, in contrast with TiO_2 [10], Cr(VI) reduction under UV irradiation is not possible without the presence of Cit or Ox, although the energy level of the CB of nanohematite (0.0-0.6 V) is enough to reduce Cr(VI) to Cr(V) (E° = 0.55 V [44]), the first step of the reduction pathway. The small decay in the presence of alcohols (inset of Fig. 1) can be attributed to the homogeneous induced Cr (VI) reduction by these compounds under UV radiation (with 2-PrOH being more efficient than MeOH) [46], and which is important only at high alcohol concentrations. Indeed, the direct Cr(VI) photochemical reaction has been described to occur at low extent when Ox or Cit are present [12,14,47], but generally higher light intensities or longer irradiation times than those used here were required.

The CB position of *n*Hm precludes reduction of oxygen to superoxide radicals ($E^{\circ}_{O_2/O_2^{\bullet-}} = -0.33$ V), avoiding the possible competition of O_2 with Cr(VI) for the e_{CB}^-. However, $HO_2^{\bullet}$ (the conjugate acid) can be formed in the system by another process (Eq. (5)); additionally, it has been determined that, in comparison with $HO^{\bullet}$, H_2O_2 is the main product of the h_{VB}^+ oxidation of adsorbed H_2O and/or surface OH^- (Eqs. (3) and (4)) [17]. This should be expected, considering that the energy level of the *n*Hm VB (2.3–2.7 V) is not enough to allow water oxidation to $HO^{\bullet}$ ($E^{\circ}_{HO^{\bullet}/H_2O}$ = 2.8 V) as in the case of TiO_2 (unless there is a change of the redox potentials on the oxide surface). The holes, however, can oxidize Cit or Ox according to Eq. (8) and, in the presence of these donors, Cr(VI) reduction over *n*Hm is surprisingly fast. Although direct hole attack to adsorbed MeOH was proposed for oxidation of the alcohol in the gas phase over α-Fe_2O_3 nanoparticles [23,24], a low efficiency of hematite has been indicated, in agreement with our results in the presence of the alcohols, pointing out that a strong interaction with the semiconductor is necessary for hole attack, as suggested several years ago [18].

It has been claimed that Fe(III) either in solution or forming part of semiconductors such as iron oxides accelerates photocatalytic transformations [5,19,48–55], being Fe(II) in solution the main responsible

for the enhancement of Cr(VI) photoreduction.

$HO_2^{\cdot} + Fe(II) + H^+ \rightarrow Fe(III) + H_2O_2$

As very well known, Ox and Cit as ligands (L) form very stable Fe (III) complexes (Fe(III)-L) in solution that absorb in the UV–Vis range [56,57] (Eq. (9)). Similar complexes can be formed with the iron of the oxide surface. Fe(III)-L complexes in solution or formed through thermal dissolution of iron oxides such as *n*Hm in the presence of L (including aquo complexes) participate in CT reactions under UV–Vis irradiation, yielding $Fe(II)_{diss}$ plus oxidation products of L (Eqs. (11) and (12), [16] and references therein). In the case of iron oxides, some iron dissolution takes place derived from e_{CB}^- reduction of Fe(III) centers (Eq. (13)), which reduces the non-desired electron/hole recombination in photocatalytic reactions (e.g. [16,41,58,59]). Once Fe (II) is in solution, it reduces aqueous Cr(VI) through three successive one electron transfer steps (Eq. (14)) over the pH range of 2–10, even in oxygenated solutions and heterogeneous systems [44,60,61]. Fe(III) recomplexes until all L or Cr(VI) is consumed and $L^{\cdot +}$ quickly reacts with O_2 to generate $HO_2^{\cdot}/O_2^{\cdot -}$ (Eq. (16)), which ends in H_2O_2 (Eq. (17)). $HO_2^{\cdot}$, H_2O_2 and $L^{\cdot +}$ are also important reductants of Cr(VI), Cr (V) and Cr(IV). Alternative homogeneous Fenton or photo-Fenton reactions (Eqs. (17) and (18)) [17], that produce additional $HO^{\cdot}$ and $HO_2^{\cdot}$, take place also in the presence of Fe(III), enhancing the reduction efficiency [5].

$$Fe(III)/(\equiv)Fe(III) + L \rightarrow Fe(III)\text{-}L/(\equiv)Fe(III)\text{-}L \quad (9)$$

$$Fe(III)\text{-}L/(\equiv)Fe(III)\text{-}L \rightarrow Fe(II)_{diss} + L_{ox} \text{ (minor reaction)} \quad (10)$$

$$Fe(III)\text{-}L/(\equiv)Fe(III)\text{-}L + h\nu \rightarrow Fe(II)_{diss} + L^{\cdot +} \rightarrow Fe(II)_{diss} + L \quad (11)$$

$$Fe(III)(OH)_2^+ + h\nu \rightarrow Fe^{2+} + HO^{\cdot} + OH^- \quad (12)$$

$$Fe(III)/\equiv Fe(III) + e_{CB}^- \rightarrow Fe(II)_{diss}/\equiv Fe(II) \quad (13)$$

$$Cr(VI)/Cr(V)/Cr(IV) + Fe(II) \rightarrow Cr(V)/Cr(IV)/Cr(III) + Fe(III) \quad (14)$$

$$HO_2^{\cdot} + Fe(III) \rightarrow Fe(II) + O_2 + H^+ \quad (15)$$

$$L^{\cdot +} + O_2 \rightarrow HO_2/O_2^{\cdot +} + O_2 \rightarrow HO_2/O_2^{\cdot -} + \text{oxidation products of L} \quad (16)$$

$$HO_2^{\cdot} + Fe(II) + H^+ \rightarrow Fe(III) + H_2O_2 \quad (17)$$

$$Fe(II) + H_2O_2\ (h\nu) \rightarrow Fe(III) + OH^- + HO^{\cdot} \quad (18)$$

In Eq (14), the first electron transfer is generally taken as the rate-limiting step as indicated by Buerge and Hug, who have also established that Fe(II) in the presence of Cit or Ox is a very strong reductant of Cr (VI), the rate constants increasing with the decreasing reduction potential of the Fe(III)-L/Fe(II)-L redox couples [62]. For those cases, they proposed the following reactions:

$$Cr(VI) + Fe(II)\text{-}L \rightarrow Cr(VI)Fe(II)\text{-}L \quad (19)$$

$$Cr(VI)Fe(II)\text{-}L \rightarrow Cr(V)Fe(III)\text{-}L \quad (20)$$

$$Cr(V)Fe(III)\text{-}L \rightarrow Cr(V) + Fe(III)\text{-}L \quad (21)$$

$$Cr(V) + Fe(II)\text{-}L \rightarrow Cr(IV) + Fe(III)\text{-}L \qquad k > 10^8\ (M^{-1}\ s^{-1}) \quad (22)$$

$$Cr(IV) + L \rightarrow Cr(IV)\text{-}L \qquad k > 10^8\ (M^{-1}\ s^{-1}) \quad (23)$$

$$Fe(II)L + Cr(IV)\text{-}L \rightarrow Fe(III)\text{-}L + Cr(III)\text{-}L \qquad k > 10^8\ (M^{-1}\ s^{-1}) \quad (24)$$

The dissolved iron seen in Fig. 2(a) in the dark comes from the thermal dissolution of the iron oxide in the presence of L (Eq. (9) [16,63 and references therein]. Fe(II) in solution was never detected in these dark experiments, as the only source of Fe(II) would be reduction of Fe (III) (dissolved, complexed or of the *n*Hm structure, Eq. (10)). However, if formed, the amount of Fe(II) formed through this thermal reaction is minor, as it has never been detected in the dark experiments (Section 3.1).

The higher amount of dissolved iron found in the dark in the presence of Ox compared with the Cit system indicates that Ox is a more efficient L for iron dissolution than Cit.

Under UV–Vis irradiation, Fe(II) formation takes place in all systems with Fe(III) and L. For Ox, it is very well known that the reaction proceeds with a high quantum efficiency at acid pH ($\varphi_{FeOx} > 1$), the Fe (III)-Ox complex being active up to 510 nm [64–66]. The quantum yields at 509 nm and at 480 nm are not very different, ca. 0.9, but at higher wavelengths (e.g., 577/579 nm), the quantum yield is rather low, 0.013 [64]. Values of φ_{FeOx} have only been reported at pH 5, somewhat lower than at more acid pH [67], and no values have been reported at pH 6, indicating that this complex is probably no photoactive at that pH. In the case of Cit, the quantum yield of Fe(II) formation, φ_{FeCit}, is quite lower, i.e., 0.28 (or less) at 366 nm [65,68,69] and 436 nm [70] (see section S4 for the complete reactions). Values of φ_{FeCit} at 366 nm at pH 6 ranging 0.08-0.4 have been reported [68,69,71].

The fact that the Cr(VI) decay is much faster in the Fe(III) homogeneous system than with *n*Hm (Fig. 1) suggests that, in the heterogeneous system, Cr(VI) reduction is strongly dependent on the presence of iron in solution, and that Fe(II) species formed either on the interface or in solution would be responsible, at least in part, for the reduction. *n*Hm would serve mainly as a source of iron in solution, supported by the fact that the reduction is very low in the absence of donors or with non-complexing species as alcohols. Indeed, a decreased efficiency of the UV degradation of Ox in the presence of iron(III) has been previously observed when TiO_2 was added to the system, due to a reduction of the Fe(III)-Ox photolytic efficiency by the solid [50]. The effect of TiO_2 addition was not very important in the case of Cit [51], and it has been justified by the lower quantum yield of the Cit complex. In the present case, it is also due to the lower $[Fe_T]$ in solution when Cit was used.

The higher Cr(VI) decay in the presence of Ox compared with Cit at pH 3 under UV–Vis irradiation, either homogeneous or heterogeneous (Fig. 1) can be attributed to two main reasons: 1) a higher amount of initial Fe in the Ox system (Fig. 2); 2) the higher quantum yield of Fe(II) formation. The increase in pH from 3 to 5 observed in the Ox system, which provokes the decrease of $[Fe_T]$ (Fig. 2(a)) is due to the consumption of protons by the Cr(VI) reduction process [44]; this increase did not take place in the Cit system due to the following three reasons: 1) the higher buffer capacity of Cit at pH 3 ($pK_{a1} = 3.13$, $pK_{a2} = 4.76$ and $pK_{a3} = 6.4$ [72]) compared with that of Ox ($pK_{a1} = 1.26$ and $pK_{a2} = 4.28$ [73]); 2) to the fact that Cit is degraded to other carboxylates during the photochemical process [51,74] and not only to CO_2 as the case of Ox [50]; and 3) because the higher φ_{FeOx} compared with φ_{FeCit} causes a higher degradation of Ox at a given irradiation time.

For the heterogeneous experiments under visible light at pH 3, Fe (II) production is more important for Ox than for Cit complexes, explaining the higher initial activity. This is confirmed by the amount of iron in solution because, as also observed under UV–Vis irradiation (Fig. 2(a)), $[Fe_T]$ in solution is much higher for Ox than for Cit (Fig. 3, inset). In this case, this cannot be correlated with a higher photolysis yield because, as Fig. 3 shows, Cr(VI) removal at the end is similar for both donors and almost negligible in the homogeneous systems. The decrease in the rate for the Ox system during the run cannot be ascribed to a decrease in *n*Hm concentration by Fe(III) solubilization, as the maximum [Fe(III)] (164 μM at 180 min, see Fig. 3) is less than 6% of the initial *n*Hm. An accurate explanation to this change in the behavior of Cr(VI) reduction under these conditions cannot be given without further experiments.

As observed, Cr(VI) decay on *n*Hm is dependent on pH due probably to changes in surface charge and to the amount of iron dissolved in solution. This is rather important when comparing the results at pH 3 and pH 6 under irradiation at $\lambda > 310$ nm (cf. Figs. 1 and 4), and can be explained by a low hematite photoactivity at higher pH in the presence of Cit or Ox [71,75,76]. The higher efficiency of Cit agrees with the fact

that φ_{FeCit} values, although low, have been reported at pH 6 [68,69,71] compared with the lack of results of quantum efficiency for Ox at pH > 5. Another possible explanation for the low Cr(VI) reduction for the Ox system at pH 6 can be the formation of a solid over the hematite surface that inhibits the photocatalytic reaction. In fact, the formation of insoluble β-$FeC_2O_4.2H_2O$ has been observed during the photochemical dissolution of goethite [63] and maghemite [77] at pH > 4, which explained the arrest of the dissolution at those pH. Raman spectra of the solid at the end of the run for Cit and Ox under UV–Vis (Fig. S4) indicate that some organic compound precipitated onto the *n*Hm surface but only when Ox was used; however, the identification of the solid according to Ref. [78] was not possible (see more details in section S4). The decreasing reaction rate for Cit when pH was increased from 3 to 6 may also be attributed to the deposition of $Cr(OH)_3$ or $(Cr_xFe_{1-x})(OH)_3(s)$ on the catalyst surface, as a 32% decrease in [Cr_T] in solution was observed at pH 6, while it was constant at pH 3. Similarly, a decrease of the photocatalytic reduction of Cr(VI) was also observed with TiO_2 due to the deposition of Cr(III) on the photocatalyst surface [9,47,48].

The efficiency of *n*Hm for Cr(VI) reduction in the presence of Cit and Ox as donors can be evaluated by comparison with other photocatalysts. Xu et al. [14] tested jarosite at pH 3 under UV–Vis irradiation with either Ox or Cit as donors using a light source and a photoreactor similar to those used here, and reported Cr(VI) reduction rates much lower than those obtained here (cf. Fig. 3 of [14] with Fig. 1). Testa et al. [10] evaluated Cr(VI) photocatalytic reduction with TiO_2 P25 using Ox under UV–Vis irradiation at pH 3 under similar conditions of the present work; it can be appreciated (cf. Fig. 1(a) of [10] with Fig. 1) that *n*Hm is more efficient. When Cit is used as donor, the difference between P25 [11,47] and *n*Hm is still higher (cf. Fig. 3 of [11] and Fig. 1(a) of [47] with Fig. 1), because the experiments with TiO_2 were performed at pH 2, at which Cr(VI) reduction is favored. Considering that *n*Hm is well active in both the UV and the visible region, contrarily to TiO_2, it can be concluded that, at least with Cit or Ox, *n*Hm is a better photocatalyst for Cr(VI) removal.

4.2. Photoactive species

Figs. S5 and S6 (section S5) show the spectra of Fe(III), Cr(VI), Ox, Cit, Fe(III)/Cr(VI) mixtures and Fe(III)/Cr(VI)/L mixtures under the conditions of Figs. 1 and 3. The Fe(III)-Ox complex (probably the bis- or trisoxalateferrate) shows a not well resolved band from 450 nm downwards corresponding to CT transitions with maxima about 260 nm overlapping with a strong absorption band of the ligand at 204 nm [79,80]. The Fe(III)-Cit complex shows a broad band centered at 349 nm [66,68]. The Fe(III)-L complexes do not absorb at λ > 510 nm and, due to the low absorption of light, no significant Fe(II) formation can take place at wavelengths higher than 400 nm, with the consequent low Cr(VI) reduction in the homogeneous system (Fig. 3). This explains the differences found for Cr(VI) removal in the homogeneous system under UV–Vis and Vis irradiation (cf. Figs. 1 and 3).

Figs. S7 and S8 show the spectra of the heterogeneous systems, i.e., *n*Hm in the presence of Cr(VI) and Ox or Cit and their combinations, under the conditions of Figs. 1 and 3. The spectrum of *n*Hm shows the typical features of hematite, with a sharp increase of the absorbance below 600 nm corresponding to a band gap of around 2.0 eV [16], two shoulders around 550 and 370 nm, and a sharp increase of the absorption from 330 nm in the UV region [81] (see more details of the spectrum in section S5). The spectra of the mixture of *n*Hm with Ox or Cit show a similar shape as those of the mixture of the carboxylates with Fe(III) shown in Figs. S5 and S6. The spectrum of the *n*Hm suspension containing Cr(VI) keeps the features of the Cr(VI) spectrum with the exception of an increase of the absorbance in the visible (from 400 to 600 nm). Figs S9 and S10 show the spectra of the same suspensions at pH 6, and show a much higher absorbance, probably due to changes in the aggregation of *n*Hm, which avoids the detection of clear peaks. After addition of Cr(VI) and Ox and, to a lower extent, of Cit, all the *n*Hm spectra (at pH 3 and 6, Figs. S7-S10) show a decrease on the absorbance, due probably to destabilization and aggregation of the suspension. This effect is shown in Fig. S11 for the samples prepared at pH 6, where a significant settling of solids after 15 min without stirring can be appreciated. From these spectra, it can be concluded that surface complexes between *n*Hm and Cr(VI) (Cr(VI)@*n*Hm), Cit or Ox (L@*n*Hm) are formed. Fig. S12 is the difference spectra resulting from the spectrum of the *n*Hm suspension with Cr(VI) and Ox and the sum of the individual spectra of the components taken from Figs. S7 and S8 (pH 3), while Fig. S13 is the difference spectra obtained similarly from Figs. S9 and S10 (pH 6). According to Figs. S12 and S13, CT complexes (Cr(VI)@*n*Hm and L@*n*Hm) absorb at these wavelengths at both pH conditions. The spectra and difference spectra shown in Figs. S5-S13 indicate that all absorbing species, i.e., the semiconductor, the Fe(III)-L complexes, and the Cr(VI)@*n*Hm and L@*n*Hm surface complexes could be responsible for the photocatalytic homogeneous and heterogeneous reactions under UV–Vis irradiation (λ > 310 nm) and Vis irradiation up to 610 nm, either at pH 3 and at pH 6. However, under visible irradiation (λ > 495 nm) at pH 3, Cr(VI) reduction was also possible with both ligands in the presence of the semiconductor, what was not possible in the homogeneous systems, indicating that Fe(III)-L complexes are not active species under this condition. In addition, the values of the redox potentials of MeOH and 2-PrOH to their α-hydroxyalkyl radicals ($E^{\circ}_{(MeOH^{\cdot+}/2\text{-}MeOH)}$ = 1.45 V [82] and $E^{\circ}_{(2\text{-}PrOH^{\cdot+}/2\text{-}PrOH)}$ = 0.97 V [83]) compared with those of Cit and Ox ($E^{\circ}_{(Cit^{\cdot+}/Cit)}$ = 1.6 V [75]; $E^{\circ}_{(Ox^{\cdot+}/Ox)}$ = 2.0 V [50]) indicate that the alcohols are more easily oxidized than the carboxylates. Thus, if either *n*Hm or Cr(VI)@*n*Hm were the active species, a significant Cr(VI) reduction should have been obtained in the presence of MeOH or 2-PrOH under UV–Vis irradiation. Therefore, the active species have to be the L@*n*Hm surface complexes, being their effect especially noticeable at wavelengths higher than 495 nm. Another possibility is that, due to the low mobility of the charge carriers in α-Fe_2O_3, h_{VB}^+ oxidation can only take place with strongly bound adsorbates. This would explain why *n*Hm is not active at λ > 610 nm despite the tailoring of the surface complexes L@*n*Hm and Cr(VI)/L@*n*Hm at wavelengths beyond 700 nm. It is important to remark that L@*n*Hm CT complexes can be either the primary species responsible for the light absorption or can be species attacked by h_{VB}^+, leading to similar reactions as the individual ligands (Eqs. (7) and (8)).

5. Conclusions

With *n*Hm as semiconductor and in the presence of Cit or Ox, the system provides a cheap and easy method for the elimination of Cr(VI) in wastewaters under UV–Vis and visible irradiation. At pH 3 and λ ≥ 310 nm, the reaction was faster with Ox and the semiconductor, and all the complexes between dissolved Fe(III) and the ligands can be responsible for the reductive reaction; this includes the Cr(VI)@*n*Hm and L@*n*Hm CT complexes. In contrast, under visible light, only the L@*n*Hm CT complexes contribute to Cr(VI) reduction.

The role of the donor is key for the efficiency as, when no donor or non-complexing donors as MeOH and 2-PrOH were used, no significant Cr(VI) reduction was observed. The activity is dependent on the nature of the donor and on pH.

At λ > 495 nm and pH 3, although the decay is negligible in the homogeneous systems with Fe(III), a good Cr(VI) transformation took place with *n*Hm and both Ox and Cit, but at a lower rate than under UV light. At λ > 610 nm, no Cr(VI) transformation took place over *n*Hm.

At pH 6 and UV–Vis irradiation, a good Cr(VI) decay was obtained with Cit in the presence of *n*Hm, and some Cr(VI) transformation was found with Cit under Vis light. At both wavelengths, the reaction was negligible when Ox was used.

Mechanisms taking place under the different conditions have been proposed, including the role of surface charge transfer complexes formed over *n*Hm.

In future works, the effect at other pH values, such as 4, 5 and 7 will be analyzed, and results of real wastewaters will be included to provide insights on the real field application of this study.

As already proved with TiO_2 as photocatalyst [9], the Cr(VI)-reduction system in the presence of the ligands can serve also as a testing method for the photocatalytic activity of hematite materials. The system provides the advantages of the use of visible (solar) light, without deposition of Cr(III) on the surface of the photocatalyst in contrast with TiO_2.

Two additional remarks must be given. First, Fe dissolution from *n*Hm should still be evaluated especially for potential reuse of the photocatalyst. Secondly, the formed soluble Cr(III)-complexes with organic acids are prone to reoxidation to the toxic Cr(VI), a fact that must be controlled with respect to the toxicity of the treated waters [55,84–86].

Acknowledgements

This work was partially supported by Agencia Nacional de Promoción Científica y Tecnológica of Argentina, PICT-0463 and PICT-208 grants and by the Scientific and Technological Cooperation Argentina-GermanyBMBF/MINCYT ARG 07/005.

Appendix A. Supplementary data

Supplementary material related to this article can be found, in the online version, at doi:https://doi.org/10.1016/j.apcatb.2018.09.059.

References

[1] WHO, Guidelines for Drinking-Water Quality, Available at: 4th ed., World Health Organization, Geneva, 2011, p. 340 (Accessed 25 April 2018), http://whqlibdoc.who.int/publications/2011/9789241548151_eng.pdf.

[2] M. Owlad, M.K. Aroua, W.A.W. Daud, S. Baroutian, Removal of hexavalent chromium-contaminated water and wastewater: a review, Water Air Soil Pollut. 200 (2009) 59–78.

[3] M.I. Litter, Last advances on TiO_2-photocatalytic removal of chromium, uranium and arsenic, Curr. Opin. Green Sustain. Chem. 6 (2017) 150–158.

[4] C.E. Barrera-Díaz, V. Lugo-Lugo, B. Bilyeu, A review of chemical, electrochemical and biological methods for aqueous Cr(VI) reduction, J. Hazard. Mater. 223–224 (2012) 1–12.

[5] M.I. Litter, Heterogeneous photocatalysis transition metal ions in photocatalytic system, Appl. Catal. B: Environ. 23 (1999) 89–114.

[6] M.I. Litter, Treatment of chromium, mercury, lead, uranium, and arsenic in water by heterogeneous photocatalysis, Adv. Chem. Eng. 36 (2009) 37–67.

[7] M.I. Litter, N. Quici, B.I. Kharisov, O.V. Kharissova, H.V. Rasika Dias (Eds.), Nanomaterials for Environmental Protection, John Wiley & Sons, Hoboken (NJ), 2014, pp. 143–167 Chap. 9.

[8] M.I. Litter, Mechanisms of removal of heavy metals and arsenic from water by TiO_2-heterogeneous photocatalysis, Pure Appl. Chem. 87 (2015) 557–568.

[9] M.I. Litter, N. Quici, J.M. Meichtry, V.N. Montesinos, Photocatalytic treatment of inorganic materials with TiO_2 nanoparticles, in: H.S. Nalwa (Ed.), Encyclopedia of Nanoscience and Nanotechnology, vol. 29, American Scientific Publishers, Valencia, California, 2018, pp. 303–336.

[10] J.J. Testa, M.A. Grela, M.I. Litter, Heterogeneous photocatalytic reduction of chromium (VI) over TiO_2 particles in the presence of oxalate. Involvement of Cr(V) species, Environ. Sci. Technol. 38 (2004) 1589–1594.

[11] J.M. Meichtry, M. Brusa, G. Mailhot, M.A. Grela, M.I. Litter, Heterogeneous photocatalysis of Cr(VI) in the presence of citric acid over TiO_2 particles: relevance of Cr(V)-citrate complexes, Appl. Catal. B: Environ. 71 (2007) 101–107.

[12] L. Yang, Y. Xiao, S. Liu, Y. Li, Q. Cai, S. Luo, G. Zeng, Photocatalytic reduction of Cr (VI) on WO_3 doped long TiO_2 nanotube arrays in the presence of citric acid, Appl. Catal. B: Environ. 94 (2010) 142–149.

[13] J.M. Meichtry, Tratamiento de Cr(VI) por Fotocatálisis Heterogénea con TiO_2, Doctoral Thesis, University of Buenos Aires, 2011.

[14] Z. Xu, S. Bai, J. Liang, L. Zhou, Y. Lan, Photocatalytic reduction of Cr(VI) by citric and oxalic acids over biogenetic jarosite, Mater. Sci. Eng. C 33 (2013) 2192–2196.

[15] Y. Di Iorio, E. San Román, M.I. Litter, M.A. Grela, Photoinduced reactivity of strongly coupled TiO_2 ligands under visible irradiation. An examination of Alizarin Red @TiO_2 nanoparticulate system, J. Phys. Chem. C 112 (2008) 16532–16538.

[16] M.I. Litter, M.A. Blesa, Photodissolution of iron oxides IV: a comparative study on the photodissolution of hematite, magnetite and maghemite in EDTA media, Can. J. Chem. 70 (1992) 2502–2510.

[17] C. Baumanis, J.Z. Bloh, R. Dillert, D.W. Bahnemann, Hematite photocatalysis: dechlorination of 2,6-dichloroindophenol and oxidation of water, J. Phys. Chem. C 115 (2011) 25442–25450.

[18] C. Kormann, D.W. Bahnemann, M.R. Hoffmann, Environmental photochemistry: is iron oxide (hematite) an active photocatalyst? A comparative study: α-Fe_2O_3, ZnO, TiO_2, J. Photochem. Photobiol. A 48 (1989) 161–169.

[19] C. Guillard, C. Hoang-Van, P. Pichat, F. Marme, Laboratory study of the respective roles of ferric oxide and released or added ferric ions in the photodegradation of oxalic acid in aerated water, J. Photochem. Photobiol. A 89 (1995) 221–227.

[20] M. Mishra, D.-M. Chun, α-Fe_2O_3 as a photocatalytic material: a review, Appl. Catal. A 498 (2015) 126–141.

[21] J. Bandara, J.A. Mielczarski, A. Lopez, J. Kiwi, 2. Sensitized degradation of chlorophenols on iron oxides induced by visible light. Comparison with titanium oxide, Appl. Catal. B 34 (2001) 321–333.

[22] H. Xie, Y. Li, S. Jin, J. Han, X. Zhao, Facile fabrication of 3D-ordered macroporous nanocrystalline iron oxide films with highly efficient visible light induced photocatalytic activity, J. Phys. Chem. C 114 (2010) 9706–9712.

[23] Z. Zhang, M.D.F. Hossain, T. Miyazaki, T. Takahashi, Gas phase photocatalytic activity of ultrathin Pt layer coated on α-Fe_2O_3 films under visible light illumination, Environ. Sci. Technol. 44 (2010) 4741–4746.

[24] H. Zhang, H. Ming, S. Lian, H. Huang, H. Li, L. Zhang, Y. Liu, Z. Kang, S.-T. Lee, Fe_2O_3/carbon quantum dots complex photocatalysts and their enhanced photocatalytic activity under visible light, Dalton Trans. 40 (2011) 10822–10825.

[25] Y. Shi, H. Li, L. Wang, W. Shen, H. Chen, Novel αFe_2O_3/CdS Cornlike Nanorods with Enhanced Photocatalytic Performance, ACS Appl. Mater. Interfaces 4 (2012) 4800–4806.

[26] P. Xu, G.M. Zeng, D.L. Huang, C.L. Feng, S. Hu, M.H. Zhao, C. Lai, Z. Wei, C. Huang, G.X. Xie, Z.F. Liu, Use of iron oxide nanomaterials in wastewater treatment: a review, Sci. Total Environ. 424 (2012) 1–10.

[27] H. Li, Q. Zhao, X. Li, Z. Zhu, M. Tade, S. Liu, Fabrication, characterization, and photocatalytic property of α-Fe_2O_3/graphene oxide composite, J. Nanopart. Res. 15 (2013) 1670–1681.

[28] L. He, L. Jing, Z. Li, W. Sun, C. Liu, Enhanced visible photocatalytic activity of nanocrystalline α-Fe_2O_3 by coupling phosphate functionalized graphene, RSC Adv. 3 (2013) 7438–7444.

[29] G.K. Pradhan, D.K. Padhi, K. Parida, Fabrication of α-Fe_2O_3 Nanorod/RGO composite: a novel hybrid photocatalyst for phenol degradation, ACS Appl. Mater. Interfaces 5 (2013) 9101–9110.

[30] W. Sun, Q. Meng, L. Jing, D. Liu, Y. Cao, Facile synthesis of surface-modified nanosized α-Fe_2O_3 as efficient visible photocatalysts and mechanism insight, J. Phys. Chem. C 117 (2013) 1358–1365.

[31] D. Barreca, G. Carraro, A. Gasparotto, Ch. Maccato, F. Rossi, G. Salviati, M. Tallarida, Ch. Das, F. Fresno, D. Korte, U. Lavrencic Stangar, M. Franko, D. Schmeisser, Surface functionalization of nanostructured Fe_2O_3 polymorphs: from design to light-activated applications, ACS Appl. Mater. Interfaces 5 (2013) 7130–7138.

[32] H. Liang, X. Xu, W. Chen, B. Xu, Z. Wang, Facile synthesis of hematite nanostructures with controlled hollowness and porosity and their comparative photocatalytic activities, Cryst. Eng. Comm. 16 (2014) 959–963.

[33] S. Han, L. Hu, Z. Liang, S. Wageh, A.A. Al-Ghamdi, Y. Chen, X. Fang, One-step hydrothermal synthesis of 2d hexagonal nanoplates of α-Fe_2O_3/graphene composites with enhanced photocatalytic activity, Adv. Funct. Mater. 24 (2014) 5719–5727.

[34] R. Sugranez, J. Balbuena, M. Cruz-Yusta, F. Martín, J. Morales, L. Sánchez, Efficient behaviour of hematite towards the photocatalytic degradation of NO_x gases, Appl. Catal. B 165 (2015) 529–536.

[35] C. Ruales-Lonfat, J.F. Barona, A. Sienkiewicz, M. Bensimon, J. Vélez-Colmenares, N. Benítez, C. Pulgarín, Iron oxides semiconductors are efficient for solar water disinfection: a comparison with photo-Fenton processes at neutral pH, Appl. Catal. B 166–167 (2015) 497–508.

[36] J. Lei, C. Liu, F. Li, X. Li, S. Zhou, T. Liu, M. Gu, Q. Wu, Photodegradation of orange I in the heterogeneous iron oxide–oxalate complex system under UVA irradiation, J. Hazard. Mater. B 137 (2006) 1016–1024.

[37] H. Mekatel, S. Amokrane, B. Bellal, M. Trari, D. Nibou, Photocatalytic reduction of Cr(VI) on nanosized Fe_2O_3 supported on natural Algerian clay: characteristics, kinetic and thermodynamic study, Chem. Eng. J. 200–202 (2012) 611–618.

[38] Y. Du, Z. Tao, J. Guan, Z. Sun, W. Zeng, P. Wen, K. Ni, J. Ye, S. Yang, P. Du, Y. Zhu, Microwave-assisted synthesis of hematite/activated graphene composites with superior performance for photocatalytic reduction of Cr(VI), RSC Adv. 5 (2015) 81438–81444.

[39] V.N. Montesinos, N. Quici, E.B. Halac, A.G. Leyva, G. Custo, G. Zampieri, S. Bengio, M.I. Litter, Highly efficient removal of Cr(VI) from water with nanoparticulated zerovalent iron: understanding the Fe(III)–Cr(III) passive outer layer structure, Chem. Eng. J. 244 (2014) 569–575.

[40] V.N. Montesinos, N. Quici, M.I. Litter, Visible light enhanced Cr(VI) removal from aqueous solution by nanoparticulated zerovalent iron, Catal. Commun. 46 (2014) 57–60.

[41] B.C. Faust, M.R. Hoffmann, D.W. Bahnemann, Photocatalytic oxidation of sulfur dioxide in aqueous suspensions of α-Fe_2O_3, J. Phys. Chem. 93 (1989) 6371–6381.

[42] P. Urone, Standard Test Methods for Chromium in Water, APHA AWWA, ASTM Standards D, (1999), pp. 1687–1692.

[43] E.B. Sandell, Colorimetric Determination of Trace Metals, Interscience Publishers Inc., New York, 1959, pp. 537–542.

[44] I.J. Buerge, S.J. Hug, Kinetics and pH dependence of chromium(VI) reduction by iron(II), Environ. Sci. Technol. 31 (1997) 1426–1432.

[45] F.J. Millero, Effect of ionic interactions on the oxidation of Fe(II) and Cu(I) in natural waters, Marine Chem. 28 (1989) 1–18.

[46] P. Mytych, A. Karocki, Z. Stasicka, Mechanism of photochemical reduction of chromium(VI) by alcohols and its environmental aspects, J. Photochem. Photobiol.

A 160 (2003) 163–170.
[47] V.N. Montesinos, C. Salou, J.M. Meichtry, C. Colbeau-Justin, M.I. Litter, Role of Cr (III) deposition during the photocatalytic transformation of hexavalent chromium and citric acid over commercial TiO_2 samples, Photochem. Photobiol. Sci. 15 (2016) 228–234.
[48] J. Muñoz, X. Domenech, TiO_2 catalysed reduction of Cr-(VI) in aqueous solutions under ultraviolet illumination, J. Appl. Electrochem. 20 (1990) 518–521.
[49] M.I. Litter, J.A. Navío, Comparison of the photocatalytic efficiency of TiO_2, iron oxides and mixed Ti(IV)/Fe(III) oxides. Photodegradation of oligocarboxylic acids, J. Photochem. Photobiol. A: Chem. 84 (1994) 183–193.
[50] N. Quici, M.E. Morgada, G. Piperata, P.A. Babay, R.T. Gettar, M.I. Litter, Oxalic acid destruction at high concentrations by combined heterogeneous photocatalysis and photo-Fenton processes, Catal. Today 101 (2005) 253–260.
[51] N. Quici, M.E. Morgada, R.T. Gettar, M. Bolte, M.I. Litter, Photocatalytic degradation of citric acid under different conditions: TiO_2 heterogeneous photocatalysis against homogeneous photolytic processes promoted by Fe(III) and H_2O_2, Appl. Catal. B 71 (2007) 117–124.
[52] Y.-g. Liu, X.-j. Hu, H. Wang, A.-w. Chen, S.-m. Liu, Y.-m. Guo, Y. He, X. Hu, J. Li, S.-h. Liu, Y.-q. Wang, L. Zhou, Photoreduction of Cr(VI) from acidic aqueous solution using TiO_2-impregnated glutaraldehyde-crosslinked alginate beads and the effects of Fe(III) ions, Chem. Eng. J. 226 (2013) 131–138.
[53] B.A. Marinho, R.O. Cristóvão, J.M. Loureiro, R.A.R. Boaventura, V.J.P. Vilar, Solar photocatalytic reduction of Cr(VI) over Fe(III) in the presence of organic sacrificial agents, Appl. Catal. B 192 (2016) 208–219.
[54] R. Liu, X. Zhu, B. Chen, A new insight of graphene oxide Fe(III) complex photochemical behaviors under visible light irradiation, Sci. Rep. 7 (2017) 40711, https://doi.org/10.1038/srep40711.
[55] G. Subramanian, G.S.S. Kumar, V. Ravi, N.R. Sundaresan, G. Madras, Photochemical detoxification of Cr (VI) using iron and saccharic acid: insights from cytotoxic and genotoxic assays, Environ. Sci.: Water Res. Technol. 4 (2018) 1152–1162.
[56] Y. Zuo, J. Hoigné, Formation of hydrogen peroxide and depletion of oxalic acid in atmospheric water by photolysis of iron(III)-oxalato complexes, Environ. Sci. Technol. 26 (1992) 1014–1022.
[57] D. Nahsheng, W. Feng, L. Fan, X. Mei, Ferric citrate-induced photodegradation of dyes in aqueous solutions, Chemosphere 36 (1998) 3101–3112.
[58] C. Pulgarin, J. Kiwi, Iron oxide-mediated degradation, photodegradation, and biodegradation of aminophenols, Langmuir 11 (1995) 519–526.
[59] M.I. Litter, J.A. Navío, Photocatalytic properties of iron-doped titania semiconductors, J. Photochem. Photobiol. A 98 (1996) 171–181.
[60] L.E. Eary, D. Ral, Chromate removal from aqueous wastes by reduction with ferrous ion, Environ. Sci. Technol. 22 (1988) 972–977.
[61] I.J. Buerge, S.J. Hug, Influence of mineral surfaces on chromium(VI) reduction by iron(II), Environ. Sci. Technol. 33 (1999) 4285–4291.
[62] I.J. Buerge, S.J. Hug, Influence of organic ligands on chromium(VI) reduction by iron(II), Environ. Sci. Technol. 32 (1998) 2092–2099.
[63] R.M. Cornell, P.W. Schindler, Photochemical dissolution of goethite in acid/oxalate solution, Clays Clay Miner. 35 (1987) 347–352.
[64] G. Hatchard, C.A. Parker, A new sensitive chemical actinometer. II. Potassium ferrioxalate as a standard chemical actinometer, Proc. R. Soc. London A 235 (1956) 518–536.
[65] I.P. Pozdnyakov, O.V. Kel, V.F. Plyusnin, V.P. Grivin, N.M. Bazhin, New insight into photochemistry of ferrioxalate, J. Phys. Chem. A 112 (2008) 8316–8322.
[66] I.P. Pozdnyakov, A.V. Kolomeets, V.F. Plyusnin, A.A. Melnikov, V.O. Kompanets, S.V. Chekalin, N. Tkachenko, H. Lemmetyinen, Photophysics of Fe(III)–tartrate and Fe(III)–citrate complexes in aqueous solutions, Chem. Phys. Lett. 530 (2012) 45–48.
[67] C. Weller, S. Horn, H. Herrmann, Effects of Fe(III)-concentration, speciation, excitation-wavelength and light intensity on the quantum yield of iron(III)-oxalato complex photolysis, J. Photochem. Photobiol. A 255 (2013) 41–49.
[68] H.B. Abrahamson, A.B. Rezvani, J.G. Brushmiller, Photochemical and spectroscopic studies of complexes of iron(III) with citric acid and other carboxylic acids, Inorg. Chim. Acta 226 (1994) 117–127.
[69] O. Abida, M. Kolar, J. Jirkovsky, G. Mailhot, Degradation of 4-chlorophenol in aqueous solution photoinduced by Fe(III)–citrate complex, Photochem. Photobiol. Sci. 11 (2012) 794–802.
[70] B.C. Faust, R.G. Zepp, Photochemistry of aqueous iron(III)-polycarboxylate complexes: roles in the chemistry of atmospheric and surface waters, Environ. Sci. Technol. 27 (1993) 2517–2522.
[71] S.J. Hug, L. Canonica, M. Wegelin, D. Gechter, U. Von Gunte, Solar oxidation and removal of arsenic at circumneutral pH in iron containing waters, Environ. Sci. Technol. 35 (2001) 2114–2121.
[72] A.E. Martell, R.M. Smith, Critical Stability Constants vol. 5, Plenum Press, New York and London, 1974, p. 329.
[73] R.M. Kettler, D.A. Palmer, D.J. Wesolowski, Dissociation quotients of oxalic acid in aqueous sodium chloride media to 175 °C, J. Sol. Chem. 20 (1991) 905–927.
[74] J.M. Meichtry, N. Quici, G. Mailhot, M.I. Litter, Heterogeneous photocatalytic degradation of citric acid over TiO_2 II. Mechanism of citric acid degradation, Appl. Catal. B 102 (2011) 555–562.
[75] S.J. Hug, H.-U. Laubscher, Iron(III) catalyzed photochemical reduction of chromium(VI) by oxalate and citrate in aqueous solutions, Environ. Sci. Technol. 31 (1997) 160–170.
[76] G. Zhou, J. Guo, G. Zhou, X. Wan, H. Shi, Photodegradation of Orange II using waste paper sludge-derived heterogeneous catalyst in the presence of oxalate under ultraviolet light emitting diode irradiation, J. Environ. Sci. 47 (2016) 63–70.
[77] M.I. Litter, E.C. Baumgartner, G.A. Urrutia, M.A. Blesa, Photodissolution of iron oxides. 3. Interplay of photochemical and thermal processes in maghemite/carboxylic acid systems, Environ. Sci. Technol. 25 (1991) 1907–1913.
[78] H.G.M. Edwards, N.C. Russell, Vibrational spectroscopic study of iron(II) and iron (III) oxalates, J. Mol. Struct. 443 (1998) 223–231.
[79] S.J. Hug, H.-U. Laubscher, Iron(III) catalyzed photochemical reduction of chromium(VI) by oxalate and citrate in aqueous solutions, Environ. Sci. Technol. 31 (1997) 160–170.
[80] I.P. Pozdnyakov, O.V. Kel, V.F. Plyusnin, V.P. Grivin, N.M. Bazhin, New insight into photochemistry of ferrioxalate, J. Phys. Chem. A 112 (2008) 8316–8322.
[81] L.A. Marusak, R. Messier, W.B. White, Optical absorption spectrum of hematite, α-Fe_2O_3 near IR to UV, Phys. Chem. Solids 41 (1980) 981–984.
[82] C. Wang, R. Pagel, D.W. Bahnemann, J.K. Dohrmann, Quantum yield of formaldehyde formation in the presence of colloidal TiO_2-based photocatalysts: effect of intermittent illumination, platinization, and deoxygenation, J. Phys. Chem. B 108 (2004) 14082–14092.
[83] S.-G. Sun, D.- Yang, Z.-W. Tian, In situ FTIR studies on the adsorption and oxidation of n-propanol and i-propanol at a platinum electrode in sulphuric acid solutions, J. Electroanal. Chem. 289 (1990) 177–187.
[84] J. Li, J. Bai, K. Huang, B. Zhou, Y. Wang, X. Hu, Removal of trivalent chromium in the complex state of trivalent chromium passivation wastewater, Chem. Eng. J. 236 (2014) 59–65.
[85] Y. Ye, Z. Jiang, Z. Xu, X. Zhang, D. Wang, L. Lv, B. Pan, Efficient removal of Cr(III)-organic complexes from water using UV/Fe(III) system: negligible Cr(VI) accumulation and mechanism, Water Res. 126 (2017) 172–178.
[86] D. Wang, S. He, C. Shan, Y. Ye, H. Ma, X. Zhang, W. Zhang, B. Pan, Chromium speciation in tannery effluent after alkaline precipitation: isolation and characterization, J. Hazard. Mater. 316 (2016) 169–177.